



Adaptive fixed-time tracking control for nonlinear systems subject to asymmetric input saturation[☆]

Ya-Feng Zhou^a, Shan-Liang Zhu^{a,b,c}, Wei Zhao^a, Yu-Qun Han^{a,b,c,*}

^a School of Mathematics and Physics, Qingdao University of Science and Technology, Qingdao, China

^b The Research Institute for Mathematics and Interdisciplinary Sciences, Qingdao University of Science and Technology, Qingdao, China

^c Qingdao Innovation Center of Artificial Intelligence Ocean Technology, Qingdao 266061, China

ARTICLE INFO

Recommended by T. Parisini

Keywords:

Fixed-time
Asymmetric input saturation
Multi-dimensional Taylor network
Backstepping technique
Nonlinear systems

ABSTRACT

For nonlinear systems with asymmetric input saturation, an adaptive fixed-time control strategy via multi-dimensional Taylor network (MTN) is proposed to effectively solve the tracking control problem. Firstly, the Gaussian error function and the differential mean value theorem are used to simulate the asymmetric input saturation model, that is, the nonlinear model is transformed into a linear model with a bounded perturbation. Secondly, MTNs are applied to control the design process, which approximate the nonlinear structures with linear combination of polynomials. Thirdly, in addition to the tracking error converging to an arbitrarily small neighborhood around the origin within a fixed time, the proposed control scheme not only guarantees that any signal in the controlled system remains bounded, but also avoids the problem of finite-time control relying on the initial state. Finally, three examples are used to validate the feasibility and superiority of the scheme.

1. Introduction

In recent years, nonlinear system control has attracted more and more attention and many meaningful research have been reported (Jayaprakash & Mackunis, 2022; Lensvelt, Speetjens, & Nijmeijer, 2022; McAllister & Rawlings, 2023; Mesbah, 2016; Wu, Jin, Liu, Yu, & Yang, 2024; Wu & Yang, 2023). Among them, the most representative is adaptive control, which can automatically adjust the controller parameters or control laws in the system to adapt to the dynamic characteristics of system objects and disturbances. However, when there is structural uncertainty rather than parameter uncertainty in the system, the traditional adaptive control cannot achieve satisfactory control results. To overcome this problem, neural networks (NNs) (Li & Xiang, 2019; Wang, Chen, Lin, Zhang, & Meng, 2018; Zhang, Ge, & Hang, 2000) and fuzzy logic systems (FLSs) (Sun, Su, Wu, & Xia, 2021; Yang, Sun, & Fang, 2022) are integrated into the framework of the backstepping approach, and NN-based or FLSs-based adaptive controllers are constructed recursively. However, the above two approximation-based adaptive control methods have certain limitations. For example, NN-based control strategy has slow convergence speed and partial minimum; FLSs-based control strategy has strong subjectivity in the selection of fuzzy rules, and the control performance is easily affected by parameter changes. To address the above concerns, a NN with a

special structure, multi-dimensional Taylor network (MTN), has been proposed (He, Zhu, Li, & Han, 2023a; Li, Han, He & Zhu, 2022; Wang, Zhu, Liu, Du, & Han, 2023b). The core idea of MTN is to approximate unknown nonlinear function by a linear combination of polynomials. As a result, MTN has the advantages of simple structure, fast convergence speed, low complexity and easy to solve. Therefore, MTN has been successfully applied to control problems of nonlinear systems, and many adaptive MTN-based control strategies have been obtained for different systems (He, Zhu, Li, & Han, 2023; Kang & Yan, 2022; Wang, Han, Lu, & Zhu, 2024; Wang, Yan, & Zheng, 2023a). Despite many developments have been achieved based on MTN, fewer results focus on the dynamic performance of the nonlinear system with input constraints.

In reality, due to the mechanical design and physical limitations of practical engineering systems, the input saturation is almost inevitable. The presence of input saturation has a significant impact on system performance, even disrupting the stability of the system. Therefore, in order to eliminate the influence of input saturation on the controlled system, approximation method and compensation method have been proposed and produced substantial far-reaching outcomes (Wang & Chen, 2021; Wen, Zhou, Liu, & Su, 2011). Compared with the latter, the former has the advantages of simplifying the design complexity of the controller, and being easy to apply in practice. Therefore, the

[☆] This work was supported by the Shandong Provincial Natural Science Foundation, China (No. ZR2020QF055).

* Corresponding author at: School of Mathematics and Physics, Qingdao University of Science and Technology, Qingdao, China.

E-mail addresses: z2022090031@163.com (Y.-F. Zhou), zhushanliang@qust.edu.cn (S.-L. Zhu), zhaowei_06@163.com (W. Zhao), yuqunhan@qust.edu.cn (Y.-Q. Han).

former is widely applied to different types of nonlinear systems subject to input saturation, such as nonlinear systems (Han, Li, He, & Zhu, 2021; Li, Zhu, He & Han, 2022), large-scale nonlinear systems (Zhu & Han, 2022), stochastic nonlinear systems (Wang, Chen, Liu, Liu & Lin, 2014), and uncertain nonlinear systems (Li, Tong, & Li, 2016). However, although the above literatures addressed the control accuracy issue of the controlled systems, its control efficiency is still relatively low.

As we all know, the control strategy of the system usually needs to meet certain rapidity (Saravanan & Meenasaranya, 2018, 2022). Therefore, in order to achieve rapidity, finite time control is generated. Its advantages include strong anti-interference, short convergence time, high convergence accuracy and fast convergence speed. As a result, finite time control of nonlinear systems has been favored by scholars and achieved many brilliant results (Liu, Gao, Liu, & Tong, 2020; Wang, Wen, & Liu, 2019). However, when the initial state is unknown, the finite time control will fail, so the tracking effect cannot be achieved. In recent years, in order to overcome the limitation of finite time control dependence on initial state, the concept of fixed time stability has been proposed (Polyakov, Efimov, & Perruquetti, 2015). Its appearance compensates for the deficiency of systems with unknown initial states that cannot adopt finite time control (Zuo, 2015; Zuo, Tian, Defoort, & Ding, 2018). However, it requires any solution of the system to converge to the equilibrium point in a fixed time, which is too strict. Because of the interference and unknown parameters in the actual system, it is difficult for the system to achieve fixed time stability. In recent years, the concept of practical fixed time stability has been proposed. This concept only requires any solution of the system to converge to a sufficiently small neighborhood of the equilibrium point, greatly relaxing the conditions for fixed time control (Chen, Wang, & Liu, 2021; Liu, Yu, He, & Sun, 2021; Ning, Han, & Zuo, 2019; Tao, Fan, Fu, Wang, & Wang, 2022). Therefore, the practical fixed time stability has more practical value. However, to my knowledge, there is currently no literature that can apply adaptive multidimensional Taylor network control and fixed time control within a unified framework to nonlinear systems with input saturation.

Based on the above analysis, the problem of adaptive MTN fixed-time tracking control for a class of nonlinear systems with asymmetric input saturation is discussed in this paper. Compared with existing achievements, the main innovations of this article include:

(1) For tracking control of nonlinear systems with asymmetric input saturation, a fixed time MTN control programme is presented for the first time. In this scheme, the output of the system can achieve tracking of the desired target when the initial state is unknown. The scheme has the advantages of easy application, low computational complexity, simple structure and no dependence on the initial state.

(2) Compared with Gao, Sun, Wen, and Wang (2017) and Li, Bai, Zhou, Lu, and Wang (2017), a fixed time control scheme is developed for nonlinear systems with input saturation. Therefore, the control scheme proposed in this paper has shorter convergence time and faster convergence speed. Compared with Tao et al. (2022), the control scheme in this paper not only adopts fixed time control, but also considers the input saturation problem, which improves the control accuracy. In addition, authors in Sun, Gao, and Zhao (2022) has developed a finite time control scheme for nonlinear systems with input saturation. Although this scheme has strong anti-interference, due to its dependence on the initial state, it is far from the practical application range of fixed time control schemes.

2. Preliminaries and formulation

2.1. Fixed-time theory

The following nonlinear system is considered

$$\dot{x}(t) = f(x(t)) \quad (1)$$

where $x(t) \in R^n$ and $f(\cdot)$ represent system state vector and continuous nonlinear function, respectively. At the same time, $x(0) = x_0$ and $f(0) = 0$.

Definition 1 (Xu et al., 2023). The equilibrium point $x(0) = x_0$ of system (1) is said to be practical fixed-time stable if for any $t \geq T_a(x_0)$ and $\varepsilon > 0$, such that $\|x(t, x_0)\| \leq \varepsilon$ holds, where $T_a(x_0)$ is the certain upper bound of the convergence time T and $t \geq T_a(x_0)$ does not depend on the initial state of the system.

Lemma 1 (Ba, Li, & Tong, 2019). The system (1) is practical fixed-time stable, if there exists a Lyapunov function $V(x)$ satisfies

$$\dot{V}(x) \leq -\mu_1 V^h(x) - \mu_2 V^\lambda(x) + \Theta \quad (2)$$

where $\mu_1 > 0$, $\mu_2 > 0$, $0 < h < 1$, $\lambda > 1$, $0 < \Theta < \infty$ are constants. Furthermore, its settling-time $T_a(x_0)$ is estimated to be

$$T_a(x_0) \leq \frac{1}{\mu_1 \varpi (1-h)} + \frac{1}{\mu_2 \varpi (\lambda-1)} \quad (3)$$

where $0 < \varpi < 1$ is constant. Moreover, the residual set of the solution of system (1) is given by

$$x \in \left\{ V(x) \leq \min \left\{ \left(\frac{\Theta}{(1-\varpi)\mu_1} \right)^{\frac{1}{h}}, \left(\frac{\Theta}{(1-\varpi)\mu_2} \right)^{\frac{1}{\lambda}} \right\} \right\} \quad (4)$$

The following necessary lemmas are given, which play an important role in the design of the controller.

Lemma 2 (Wang & Lin, 2015). The following inequality holds, for $\forall s \in R$,

$$0 \leq |s| < \tau + \frac{s^2}{\sqrt{s^2 + \tau^2}} \quad (5)$$

where $\tau > 0$ is a constant.

Lemma 3 (Jin, 2019). For $\beta_i \in R, i = 1, 2, \dots, n$ and $\iota \in (0, 1]$, the following formula is obtained

$$\left(\sum_{k=1}^n |\beta_k| \right)^\iota \leq \sum_{k=1}^n |\beta_k|^\iota \quad (6)$$

Lemma 4 (Jin, 2019). For $\rho_i \geq 0$, the following inequality holds

$$\left(\sum_{k=1}^n \rho_k \right)^2 \leq n \sum_{k=1}^n \rho_k^2 \quad (7)$$

Lemma 5 (Wang, Chen, & Liu, 2021). For $o_1 > 0$, $o_2 > 0$, $o_3 > 0$, $\gamma_1 \geq 0$, $\gamma_2 \geq 0$, $\gamma_3 \geq 0$, the following inequality is true

$$\gamma_1^{o_1} \gamma_2^{o_2} \gamma_3 \leq \frac{o_2}{o_1 + o_2} \times \left[\frac{o_1}{o_3(o_1 + o_2)} \right]^{\frac{o_1}{o_2}} \gamma_2^{o_1 + o_2} \gamma_3^{\frac{o_1 + o_2}{o_2}} + o_3 \gamma_1^{o_1 + o_2} \quad (8)$$

Lemma 6 (Wang, Chen & Lin, 2014). For any $\forall \omega_1, \omega_2 \in R$, the following inequality is true

$$\omega_1 \omega_2 \leq \frac{\zeta^{\epsilon_1}}{\epsilon_1} |\omega_1|^{\epsilon_1} + \frac{1}{\epsilon_2 \zeta^{\epsilon_2}} |\omega_2|^{\epsilon_2} \quad (9)$$

where $\zeta > 0$, $\epsilon_1 > 1$, $\epsilon_2 > 1$ and $(\epsilon_1 - 1)(\epsilon_2 - 1) = 1$.

2.2. Problem description

In this paper, a class of nonlinear systems with asymmetric input saturation is studied, their mathematical expressions can be described

as follows

$$\begin{cases} \dot{x}_i = g_i(\bar{x}_i) x_{i+1} + f_i(\bar{x}_i) \\ i = 1, 2, \dots, n-1 \\ \dot{x}_n = g_n(\bar{x}_n) u(v) + f_n(\bar{x}_n) \\ y = x_1 \end{cases} \quad (10)$$

where x_1, x_2, \dots, x_n are the system states, $\bar{x}_i = [x_1, x_2, \dots, x_i]^T \in R^i$, for $i = 1, 2, \dots, n$. y indicates the system output. $f_i(\cdot)$ and $g_i(\cdot)$ represent unknown nonlinear functions with $f_i(0) = 0$. $u(v) \in R$ is the system input of (10). Furthermore, the input signal $u(v) \in R$ subjects to saturation nonlinearity can be described as follows

$$u(v) = \begin{cases} S, & v \geq S \\ v, & I < v < S \\ I, & v \leq I \end{cases} \quad (11)$$

where v is the input of saturation model, $S > 0$ and $I < 0$ represent the supremum and infimum of $u(v)$, respectively.

The main work of this article is to develop an adaptive fixed time controller to ensure that the system is practical fixed time stable, thereby achieving the following two control objectives:

- (1) all signals in the closed-loop controlled system remain bounded;
- (2) system output y can track the given control target y_d and the tracking error of the system converges to an arbitrarily small neighborhood around the origin in a fixed time.

For the sake of controller design, the following Assumptions are needed.

Assumption 1. The tracking target y_d and its derivatives up to n are continuously bounded.

Assumption 2. The function $g_i(\cdot)$, $i = 1, \dots, n$ in system (10) satisfy the following inequality

$$0 < \underline{g}_i < |g_i(\cdot)| < \infty \quad (12)$$

where \underline{g}_i are constants. Without losing generality, $g_i(\cdot)$ are assumed to be strictly positive.

2.3. Preprocessing of asymmetric input saturation model

The presence of sharp corners in the asymmetric input saturation model, as seen in (11), reduces the smoothness of the system input. Consequently, this leads to a diminished control effect and may even result in system instability. Based on this, the Gaussian error function and the differential mean value theorem are used in this section to preprocess the saturation model.

Firstly, the following Gaussian error function is introduced to achieve the purpose of approximating the saturation model:

$$u(v) = \Re \cdot \mathfrak{F} \left(\frac{\sqrt{\pi}v}{2\Re} \right) \quad (13)$$

where $\Re = \left(S + \frac{I}{2}\right) + \left(S - \frac{I}{2}\right) \text{sign}(v)$. $\mathfrak{F}(x)$ is a Gaussian error function, whose mathematical expression is $\mathfrak{F}(x) = \frac{2}{\sqrt{\pi}} \int_0^x e^{-s^2} ds$.

Obviously, $\mathfrak{F}(x)$ is a real-valued and continuous differentiable function. Therefore, according to the differential mean value theorem, $u(v)$ can be converted to the following form

$$u(v) = cv + \Xi(v) \quad (14)$$

where $c > 0$ is a constant, $\Xi(v)$ denotes the bounded perturbation.

Assumption 3 (Ma, Ge, Zheng, & Hu, 2015). There exist constants Δ , c^- and c^+ with $\Delta > 0$, $c^- > 0$ and $c^+ > 0$, such that $c \in [c^-, c^+]$ and

$$\Xi(x) \leq \Delta \quad (15)$$

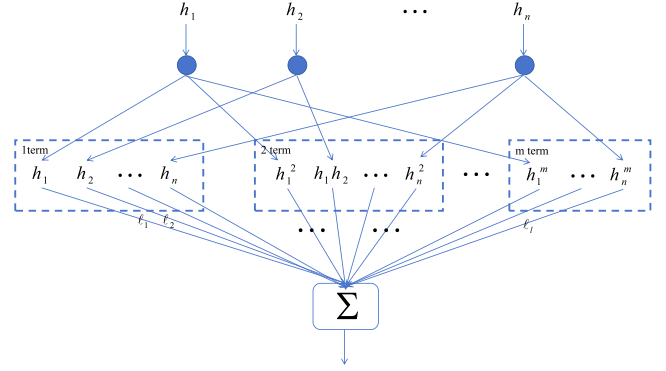


Fig. 1. The structure block diagram of MTN.

Remark 1. It should be noted that the method for dealing with input saturation in this paper is based on Han et al. (2021) and Li, Zhu et al. (2022). Since the input saturation is a typical nonlinear behavior, the nonlinear control problem can be transformed into a linear control problem with a bounded perturbation by linear decomposition, which is convenient for controller design and analysis. This treatment is commonly found in many literatures, such as Han et al. (2021), Li, Zhu et al. (2022), Ma et al. (2015) and Wang, Chen, Liu et al. (2014).

2.4. Multi-dimensional Taylor network

In this paper, MTNs are used to approximate unknown nonlinear functions. Therefore, the following lemma is given.

Lemma 7 (Du, Zhu, Zhai, & Han, 2023; He, Zhu, Lu, & Han, 2024; Zhou et al., 2024). Assuming $Q(\varphi)$ is a continuous nonlinear function defined in a compact set Ω_φ , for any constant $\varepsilon > 0$, there exists a MTN with an approximation error of $\delta(\varphi)$ that satisfies

$$Q(\varphi) = \theta^T P_{m_n}(\varphi) + \delta(\varphi), |\delta(\varphi)| < \varepsilon \quad (16)$$

where $\varphi = [h_1, h_2, \dots, h_n]^T \in R^n$ and $\theta = [\ell_1, \ell_2, \dots, \ell_l]^T \in R^l$ represent the input vector and weight vector of MTN, respectively. $P_{m_n}(\varphi)$ is the middle layer of MTN, which can be expressed as

$$P_{m_n}(\varphi) = [h_1, \dots, h_n, h_1^2, h_1h_2, \dots, h_n^2, \dots, h_1^m, \dots, h_n^m]^T \in R^l.$$

Remark 2. Fig. 1 shows the structure of MTN. From Fig. 1, it can be seen that MTN is a three-layer neural network with a special structure. Specifically, the intermediate layer of MTN is composed of an array of polynomials, which only contains addition and multiplication. The above characteristics effectively simplifies the structure of MTN, thereby reducing the training time, improving the convergence speed, and reducing the computational complexity.

3. Main results

3.1. Controller design

Before designing the controller, the following coordinate transformation will be carried out.

$$\begin{cases} z_1 = x_1 - y_d \\ z_i = x_i - \alpha_{i-1} \end{cases} \quad (17)$$

where $i = 2, \dots, n$. α_{i-1} are the virtual controllers in the backstepping design process.

Remark 3. In order to prove the convenience of derivation, in the following design process, let the parameters $\tilde{h} = \frac{3}{4}$, $\tilde{\lambda} = 2$ in (2).

Step 1: Taking the derivative of the first equation of (17) yields

$$\dot{z}_1 = f_1 + g_1 z_2 + g_1 \alpha_1 - \dot{y}_d \quad (18)$$

For the first subsystem, the Lyapunov function is constructed as follows

$$V_1 = \frac{1}{2} z_1^2 + \frac{1}{2r_1} \tilde{\theta}_1^2 \quad (19)$$

where $r_1 > 0$ represents the constant, $\tilde{\theta}_1 = \theta_1 - \hat{\theta}_1$ denotes the approximation error.

Then, the first order derivative of the Lyapunov function V_1 is

$$\dot{V}_1 = z_1 (g_1 z_2 + g_1 \alpha_1 + \bar{f}_1) - \frac{1}{2} z_1^2 - \frac{1}{r_1} \tilde{\theta}_1 \dot{\hat{\theta}}_1 \quad (20)$$

where $\bar{f}_1 = f_1 - \dot{y}_d + \frac{1}{2} z_1$ is an unknown nonlinear function.

In line with Lemma 7, for $\forall \varepsilon_1 > 0$, there is a MTN $\theta_1^T P_{m_1}(\varphi_1)$ with bounded error $\delta_1(\varphi_1)$, such that function \bar{f}_1 satisfies the following equation

$$\bar{f}_1 = \theta_1^T P_{m_1}(\varphi_1) + \delta_1(\varphi_1), \quad |\delta_1(\varphi_1)| < \varepsilon_1 \quad (21)$$

where $\varphi_1 = [z_1]^T$.

According to Lemma 6 with $\varepsilon_1 = \varepsilon_2 = 2$ and $\zeta = 1$, the following formula can be obtained:

$$z_1 \bar{f}_1 \leq z_1 \theta_1^T P_{m_1} + \frac{1}{2} z_1^2 + \frac{1}{2} \varepsilon_1^2 \quad (22)$$

Then, substituting (22) into (20), produces

$$\dot{V}_1 \leq z_1 (g_1 z_2 + g_1 \alpha_1) + z_1 \theta_1^T P_{m_1} - \frac{1}{r_1} \tilde{\theta}_1 \dot{\hat{\theta}}_1 + \frac{1}{2} \varepsilon_1^2 \quad (23)$$

On the basis of (23), the following forms of adaptive law and virtual controller are constructed

$$\dot{\hat{\theta}}_1 = r_1 P_{m_1} z_1 - \eta_1 \hat{\theta}_1 - \frac{\xi_1}{r_1} \hat{\theta}_1^3 \quad (24)$$

$$\alpha_1 = -\frac{z_1 \check{\alpha}_1^2}{\underline{g}_1 \sqrt{z_1^2 \check{\alpha}_1^2 + \tau_1^2}} \quad (25)$$

where $\check{\alpha}_1 = -K_{11} \left(\frac{1}{2} z_1\right)^{\frac{3}{4}} - \frac{1}{z_1} \Psi_{z_1} - K_{12} \left(\frac{1}{2} z_1\right)^2 z_1^3 - \hat{\theta}_1^T P_{m_1}$. The design parameters satisfy $\eta_1 > 0$, $\xi_1 > 0$, $\tau_1 > 0$, $K_{11} > 0$ and $K_{12} > 0$. Ψ_{z_1} is defined in the following form

$$\Psi_{z_1} = \begin{cases} \left(\frac{z_1^2}{2}\right)^{\frac{3}{4}}, & |z_1| \geq \tau_{10} \\ \sum_{j=1}^n C_j (z_1^2)^j (\tau_{10}^2)^{-j+\frac{3}{4}}, & |z_1| < \tau_{10} \end{cases} \quad (26)$$

where $\tau_{10} > 0$ is a small constant and the values of the coefficients C_j , ($j = 1, 2, \dots, n$) meet with

$$\Phi \times \begin{bmatrix} C_1 \\ C_2 \\ C_3 \\ \vdots \\ C_n \end{bmatrix} = \begin{bmatrix} 1 \\ \frac{3}{4} \\ \frac{3}{4} \left(\frac{3}{4} - 1\right) \\ \vdots \\ \prod_{j=0}^{n-2} \left(\frac{3}{4} - j\right) \end{bmatrix}$$

with

$$\Phi = \begin{bmatrix} 1 & 1 & \dots & 1 & 1 \\ 1 & 2 & \dots & n-1 & n \\ 0 & 2 \cdot 1 & \dots & (n-1)(n-2) & n(n-1) \\ \vdots & \vdots & \ddots & \vdots & \vdots \\ 0 & 0 & \dots & \prod_{j=1}^{n-2} (n-1-j) & \prod_{j=0}^{n-2} (n-j) \end{bmatrix}$$

According to Lemma 2, Assumption 2 and (25), $z_1 g_1 \alpha_1$ can be reduced to the following form

$$z_1 g_1 \alpha_1 \leq -\frac{z_1^2 \check{\alpha}_1^2}{\sqrt{z_1^2 \check{\alpha}_1^2 + \tau_1^2}} < \tau_1 + z_1 \check{\alpha}_1 \quad (27)$$

By substituting (24), (27) and the expression of $\check{\alpha}_1$ into (23), \dot{V}_1 can be further written as

$$\begin{aligned} \dot{V}_1 &\leq z_1 g_1 z_2 + \tau_1 + z_1 \check{\alpha}_1 + z_1 \theta_1^T P_{m_1} \\ &\quad + \frac{1}{2} \varepsilon_1^2 - \frac{1}{r_1} \tilde{\theta}_1 \left(r_1 P_{m_1} z_1 - \eta_1 \hat{\theta}_1 - \frac{\xi_1}{r_1} \hat{\theta}_1^3 \right) \\ &\leq -K_{11} \left(\frac{1}{2} z_1\right)^{\frac{3}{4}} \Psi_{z_1} - K_{12} \left(\frac{1}{2} z_1\right)^2 z_1^4 \\ &\quad + z_1 g_1 z_2 + \frac{\eta_1}{r_1} \tilde{\theta}_1 \hat{\theta}_1 + \frac{\xi_1}{r_1^2} \tilde{\theta}_1 \hat{\theta}_1^3 + \sigma_1 \end{aligned} \quad (28)$$

where $\sigma_1 = \tau_1 + \frac{1}{2} \varepsilon_1^2 > 0$.

Case 1, when $|z_1| \geq \tau_{10} > 0$, (28) can be changed to the following form

$$\begin{aligned} \dot{V}_1 &\leq -K_{11} \left(\frac{1}{2} z_1\right)^{\frac{3}{4}} - K_{12} \left(\frac{1}{2} z_1\right)^2 + z_1 g_1 z_2 \\ &\quad + \frac{\eta_1}{r_1} \tilde{\theta}_1 \hat{\theta}_1 + \frac{\xi_1}{r_1^2} \tilde{\theta}_1 \hat{\theta}_1^3 + \sigma_1 \end{aligned} \quad (29)$$

Case 2, when $|z_1| < \tau_{10}$, (28) can be changed to the following form

$$\begin{aligned} \dot{V}_1 &\leq -K_{11} \left(\frac{1}{2} z_1\right)^{\frac{3}{4}} - K_{12} \left(\frac{1}{2} z_1\right)^2 + K_{11} \left(\frac{1}{2} z_1\right)^{\frac{3}{4}} \\ &\quad - K_{11} \left(\frac{1}{2} z_1\right)^{\frac{3}{4}} \sum_{j=1}^n C_j (z_1^2)^{\frac{3}{4}} (z_1^2)^{j-\frac{3}{4}} (\tau_{10}^2)^{-j+\frac{3}{4}} \\ &\quad + z_1 g_1 z_2 + \frac{\eta_1}{r_1} \tilde{\theta}_1 \hat{\theta}_1 + \frac{\xi_1}{r_1^2} \tilde{\theta}_1 \hat{\theta}_1^3 + \sigma_1 \\ &\leq -K_{11} \left(\frac{1}{2} z_1\right)^{\frac{3}{4}} - K_{12} \left(\frac{1}{2} z_1\right)^2 + z_1 g_1 z_2 \\ &\quad + \frac{\eta_1}{r_1} \tilde{\theta}_1 \hat{\theta}_1 + \frac{\xi_1}{r_1^2} \tilde{\theta}_1 \hat{\theta}_1^3 + \sigma_1 \\ &\quad + K_{11} \left(\frac{1}{2} z_1\right)^{\frac{3}{4}} \left[1 - \sum_{j=1}^n C_j \left(\frac{1}{\tau_{10}^2} z_1^2\right)^{j-\frac{3}{4}} \right] \end{aligned} \quad (30)$$

Denote $D = K_{11} \left(\frac{1}{2} z_1\right)^{\frac{3}{4}} \left[1 - \sum_{j=1}^n C_j \left(\frac{1}{\tau_{10}^2} z_1^2\right)^{j-\frac{3}{4}} \right]$, then D satisfies

the following inequality

$$D \leq K_{11} \left(\frac{1}{2} \tau_{10}^2\right)^{\frac{3}{4}} \left[1 + \sum_{j=1}^n |C_j| \right] \quad (31)$$

Remark 4. It can be seen from (31) that D is a bounded term, which can be regarded as a small increment of σ_1 . Therefore, for the convenience of discussion, only the Case 1 will be discussed in the subsequent theoretical analysis.

Step i ($2 \leq i \leq n-1$): Taking the derivative of z_i , the following formula is correct

$$\dot{z}_i = g_i z_{i+1} + g_i \alpha_i + f_i - \dot{\alpha}_{i-1} \quad (32)$$

On the basis of V_{i-1} , V_i is constructed and its mathematical expression is as follows

$$V_i = V_{i-1} + \frac{1}{2} z_i^2 + \frac{1}{2r_i} \tilde{\theta}_i^2 \quad (33)$$

where $r_i > 0$ represents the constant.

Then, the first order derivative of the above equation is

$$\dot{V}_i = \dot{V}_{i-1} + z_i \dot{z}_i - \frac{1}{r_i} \tilde{\theta}_i \dot{\hat{\theta}}_i \quad (34)$$

By substituting (32) into (34), the following inequality can be obtained

$$\begin{aligned} \dot{V}_i \leq & -\sum_{j=1}^{i-1} K_{j1} \left(\frac{1}{2} z_j^2\right)^{\frac{3}{4}} - \sum_{j=1}^{i-1} K_{j2} \left(\frac{1}{2} z_j^2\right)^2 \\ & + \sum_{j=1}^{i-1} \frac{\eta_j}{r_j} \tilde{\theta}_j \hat{\theta}_j + \sum_{j=1}^{i-1} \frac{\xi_j}{r_j^2} \tilde{\theta}_j \hat{\theta}_j^3 + \sigma_{i-1} \\ & + z_i (g_i z_{i+1} + g_i \alpha_i + \bar{f}_i) - \frac{1}{2} z_i^2 - \frac{1}{r_i} \tilde{\theta}_i \hat{\theta}_i \end{aligned} \quad (35)$$

where $\bar{f}_i = z_{i-1} g_{i-1} + f_i - \dot{\alpha}_{i-1} + \frac{1}{2} z_i$ denotes unknown nonlinear function.

Similarly, in line with Lemma 7, for $\forall \epsilon_i > 0$, there is a MTN $\theta_i^T P_{m_i}(\varphi_i)$ with bounded error $\delta_i(\varphi_i)$, such that function \bar{f}_i satisfies the following equation

$$\bar{f}_i = \theta_i^T P_{m_i}(\varphi_i) + \delta_i(\varphi_i), \quad |\delta_i(\varphi_i)| \leq \epsilon_i \quad (36)$$

where $\varphi_i = [z_1, z_2, \dots, z_i]^T$.

Similar to (22), the following formula can be obtained

$$z_i \bar{f}_i \leq z_i \theta_i^T P_{m_i} + \frac{1}{2} z_i^2 + \frac{1}{2} \epsilon_i^2 \quad (37)$$

The adaptive law $\hat{\theta}_i$ and the intermediate virtual controller α_i are designed as follows

$$\dot{\hat{\theta}}_i = r_i P_{m_i} z_i - \eta_i \hat{\theta}_i - \frac{\xi_i}{r_i} \hat{\theta}_i^3 \quad (38)$$

$$\alpha_i = -\frac{z_i \check{\alpha}_i^2}{g_i \sqrt{z_i^2 \check{\alpha}_i^2 + \tau_i^2}} \quad (39)$$

where $\check{\alpha}_i = -K_{i1} \left(\frac{1}{2}\right)^{\frac{3}{4}} \frac{1}{z_i} \Psi_{z_i} - K_{i2} \left(\frac{1}{2}\right)^2 z_i^3 - \hat{\theta}_i^T P_{m_i}$. The design parameters satisfy $\eta_i > 0$, $\xi_i > 0$, $\tau_i > 0$, $K_{i1} > 0$ and $K_{i2} > 0$. Ψ_{z_i} is defined in the following form

$$\Psi_{z_i} = \begin{cases} (z_i^2)^{\frac{3}{4}}, & |z_i| \geq \tau_{i0} \\ \sum_{j=1}^n C_j (z_i^2)^j (\tau_{i0}^2)^{-j+\frac{3}{4}}, & |z_i| < \tau_{i0} \end{cases} \quad (40)$$

where $\tau_{i0} > 0$ is a small constant and C_j take the same value as (26).

By adopting the same processing method as (27), the following formula can be obtained

$$z_i g_i \alpha_i < \tau_i + z_i \check{\alpha}_i \quad (41)$$

Substituting (37), (38), (41) and the expression of $\check{\alpha}_i$ into (35), we can obtain

$$\begin{aligned} \dot{V}_i \leq & -\sum_{j=1}^i K_{j1} \left(\frac{1}{2} z_j^2\right)^{\frac{3}{4}} - \sum_{j=1}^i K_{j2} \left(\frac{1}{2} z_j^2\right)^2 \\ & + \sum_{j=1}^i \frac{\eta_j}{r_j} \tilde{\theta}_j \hat{\theta}_j + \sum_{j=1}^i \frac{\xi_j}{r_j^2} \tilde{\theta}_j \hat{\theta}_j^3 + z_i g_i z_{i+1} + \sigma_i \end{aligned} \quad (42)$$

where $\sigma_i = \sigma_{i-1} + \tau_i + \frac{1}{2} \epsilon_i^2 > 0$.

Step n: By combining (10), (14), and (17), the following equation can be obtained

$$\dot{z}_n = g_n c v + g_n \Xi(v) + f_n - \dot{\alpha}_{n-1} \quad (43)$$

Similar to (33), we construct a Lyapunov function V_n as follows

$$V_n = V_{n-1} + \frac{1}{2} z_n^2 + \frac{1}{2r_n} \tilde{\theta}_n^2 \quad (44)$$

where $r_n > 0$ represents the constant.

Take the derivative of (44), and then substitute (43) into \dot{V}_n to get the following formula

$$\begin{aligned} \dot{V}_n \leq & -\sum_{j=1}^{n-1} K_{j1} \left(\frac{1}{2} z_j^2\right)^{\frac{3}{4}} - \sum_{j=1}^{n-1} K_{j2} \left(\frac{1}{2} z_j^2\right)^2 \\ & + \sum_{j=1}^{n-1} \frac{\eta_j}{r_j} \tilde{\theta}_j \hat{\theta}_j + \sum_{j=1}^{n-1} \frac{\xi_j}{r_j^2} \tilde{\theta}_j \hat{\theta}_j^3 + \sigma_{n-1} \\ & + z_n (g_n c v + g_n \Xi(v) + \bar{f}_n) \\ & - \frac{1}{2} z_n^2 - \frac{1}{r_n} \tilde{\theta}_n \hat{\theta}_n - \frac{1}{2} z_n^2 g_n^2 \end{aligned} \quad (45)$$

where $\bar{f}_n = f_n - \dot{\alpha}_{n-1} + \frac{1}{2} z_n + \frac{1}{2} z_n g_n^2 + z_{n-1} g_{n-1}$ indicates unknown nonlinear function.

According to Lemma 6 with $\epsilon_1 = \epsilon_2 = 2$ and $\zeta = 1$, and taking Assumption 3 into account, the following formula can be obtained:

$$z_n g_n \Xi(v) \leq \frac{1}{2} z_n^2 g_n^2 + \frac{1}{2} \Delta^2 \quad (46)$$

Similarly, in line with Lemma 7, for $\forall \epsilon_n > 0$, there is a MTN $\theta_n^T P_{m_n}(\varphi_n)$ with bounded error $\delta_n(\varphi_n)$, such that function \bar{f}_n satisfies the following equation

$$\bar{f}_n = \theta_n^T P_{m_n}(\varphi_n) + \delta_n(\varphi_n), \quad |\delta_n(\varphi_n)| \leq \epsilon_n \quad (47)$$

where $\varphi_n = [z_1, z_2, \dots, z_n]^T$.

According to Lemma 6 and (47), $z_n \bar{f}_n$ can be reduced to the following form

$$z_n \bar{f}_n \leq z_n \theta_n^T P_{m_n} + \frac{1}{2} z_n^2 + \frac{1}{2} \epsilon_n^2 \quad (48)$$

By substituting (46) and (48) into (45), we get

$$\begin{aligned} \dot{V}_n \leq & -\sum_{j=1}^{n-1} K_{j1} \left(\frac{1}{2} z_j^2\right)^{\frac{3}{4}} - \sum_{j=1}^{n-1} K_{j2} \left(\frac{1}{2} z_j^2\right)^2 \\ & + \sum_{j=1}^{n-1} \frac{\eta_j}{r_j} \tilde{\theta}_j \hat{\theta}_j + \sum_{j=1}^{n-1} \frac{\xi_j}{r_j^2} \tilde{\theta}_j \hat{\theta}_j^3 + \sigma_{n-1} + z_n g_n c v \\ & + \frac{1}{2} \Delta^2 + z_n \theta_n^T P_{m_n} + \frac{1}{2} \epsilon_n^2 - \frac{1}{r_n} \tilde{\theta}_n \hat{\theta}_n \end{aligned} \quad (49)$$

The adaptive law $\hat{\theta}_n$ and actual control input v are designed as follows

$$\dot{\hat{\theta}}_n = r_n P_{m_n} z_n - \eta_n \hat{\theta}_n - \frac{\xi_n}{r_n} \hat{\theta}_n^3 \quad (50)$$

$$v = -\left(\frac{|z_n| \check{\alpha}_n^2}{c - g_n \sqrt{z_n^2 \check{\alpha}_n^2 + \tau_n^2}} \right) \text{sgn}(z_n) \quad (51)$$

where $\check{\alpha}_n = -K_{n1} \left(\frac{1}{2}\right)^{\frac{3}{4}} \frac{1}{z_n} \Psi_{z_n} - K_{n2} \left(\frac{1}{2}\right)^2 z_n^3 - \hat{\theta}_n^T P_{m_n}$. The design parameters satisfy $\eta_n > 0$, $\xi_n > 0$, $\tau_n > 0$, $K_{n1} > 0$ and $K_{n2} > 0$. Ψ_{z_n} is defined in the following form

$$\Psi_{z_n} = \begin{cases} (z_n^2)^{\frac{3}{4}}, & |z_n| \geq \tau_{n0} \\ \sum_{j=1}^n C_j (z_n^2)^j (\tau_{n0}^2)^{-j+\frac{3}{4}}, & |z_n| < \tau_{n0} \end{cases} \quad (52)$$

where $\tau_{n0} > 0$ is seen as a small constant and C_j take the same value as (26).

From Lemma 2, Assumptions 2, and 3, it can be obtained that

$$z_n g_n c v \leq -\frac{z_n^2 \check{\alpha}_n^2}{\sqrt{z_n^2 \check{\alpha}_n^2 + \tau_n^2}} < \tau_n + z_n \check{\alpha}_n \quad (53)$$

Substituting (50), (53) and the expression of $\check{\alpha}_n$ into (49) can obtain

$$\begin{aligned} \dot{V}_n \leq & -\sum_{j=1}^n K_{j1} \left(\frac{1}{2} z_j^2\right)^{\frac{3}{4}} - \sum_{j=1}^n K_{j2} \left(\frac{1}{2} z_j^2\right)^2 \\ & + \sum_{j=1}^n \frac{\eta_j}{r_j} \tilde{\theta}_j \hat{\theta}_j + \sum_{j=1}^n \frac{\xi_j}{r_j^2} \tilde{\theta}_j \hat{\theta}_j^3 + \sigma_n \end{aligned} \quad (54)$$

where $\sigma_n = \sigma_{n-1} + \tau_n + \frac{1}{2} \Delta^2 + \frac{1}{2} \epsilon_n^2 > 0$.

Using Lemmas 3 and 4, the following two inequalities are reasonable

$$-\sum_{j=1}^n K_{j1} \left(\frac{1}{2} z_j^2\right)^{\frac{3}{4}} \leq -\bar{\mu}_1 \left(\sum_{j=1}^n \frac{1}{2} z_j^2\right)^{\frac{3}{4}} \quad (55)$$

$$-\sum_{j=1}^n K_{j2} \left(\frac{1}{2} z_j^2\right)^2 \leq -\frac{\bar{\mu}_2}{n} \left(\sum_{j=1}^n \frac{1}{2} z_j^2\right)^2 \quad (56)$$

where $\bar{\mu}_1 = \min \{K_{11}, K_{21}, \dots, K_{n1}\}$, $\bar{\mu}_2 = \min \{K_{12}, K_{22}, \dots, K_{n2}\}$.

According to Lemma 6, the following inequality can be derived

$$\sum_{j=1}^n \frac{\eta_j}{r_j} \tilde{\theta}_j \hat{\theta}_j \leq \sum_{j=1}^n \frac{\eta_j}{2r_j} \theta_j^2 - \sum_{j=1}^n \frac{\eta_j}{2r_j} \tilde{\theta}_j^2 \quad (57)$$

By substituting (55), (56) and (57) into (54), the following formula can be seen

$$\begin{aligned} \dot{V}_n \leq & -\bar{\mu}_1 \left(\sum_{j=1}^n \frac{1}{2} z_j^2\right)^{\frac{3}{4}} - \left(\sum_{j=1}^n \frac{\eta_j}{2r_j} \tilde{\theta}_j^2\right)^{\frac{3}{4}} \\ & - \frac{\bar{\mu}_2}{n} \left(\sum_{j=1}^n \frac{1}{2} z_j^2\right)^2 + \left(\sum_{j=1}^n \frac{\eta_j}{2r_j} \tilde{\theta}_j^2\right)^{\frac{3}{4}} \\ & + \sum_{j=1}^n \frac{\eta_j}{2r_j} \theta_j^2 - \sum_{j=1}^n \frac{\eta_j}{2r_j} \tilde{\theta}_j^2 + \sum_{j=1}^n \frac{\xi_j}{r_j^2} \tilde{\theta}_j \hat{\theta}_j^3 + \sigma_n \end{aligned} \quad (58)$$

Make $o_1 = 1 - o_2 = \frac{1}{4}$, $o_2 = \frac{3}{4}$, $o_3 = o_1 o_2^3$, $\gamma_1 = 1$, $\gamma_2 = \sum_{j=1}^n \frac{\eta_j}{2r_j} \tilde{\theta}_j^2$, $\gamma_3 = 1$, according to Lemma 5, the following formula can be obtained

$$\left(\sum_{j=1}^n \frac{\eta_j}{2r_j} \tilde{\theta}_j^2\right)^{\frac{3}{4}} \leq o_3 + \sum_{j=1}^n \frac{\eta_j}{2r_j} \tilde{\theta}_j^2 \quad (59)$$

According to the cubic formula of difference, it can be obtained that

$$\tilde{\theta}_j \hat{\theta}_j^3 = \tilde{\theta}_j \theta_j^3 - \tilde{\theta}_j^4 + 3\theta_j \tilde{\theta}_j^3 - 3\tilde{\theta}_j^2 \theta_j^2 \quad (60)$$

Substituting (59) and (60) into (58) to yield

$$\begin{aligned} \dot{V}_n \leq & -\bar{\mu}_1 \left(\sum_{j=1}^n \frac{1}{2} z_j^2\right)^{\frac{3}{4}} - \left(\sum_{j=1}^n \frac{\eta_j}{2r_j} \tilde{\theta}_j^2\right)^{\frac{3}{4}} \\ & - \frac{\bar{\mu}_2}{n} \left(\sum_{j=1}^n \frac{1}{2} z_j^2\right)^2 + \sum_{j=1}^n \frac{\eta_j}{2r_j} \theta_j^2 \\ & + \sum_{j=1}^n \frac{\xi_j}{r_j^2} \tilde{\theta}_j \theta_j^3 - \sum_{j=1}^n \frac{\xi_j}{r_j^2} \tilde{\theta}_j^4 + \sum_{j=1}^n \frac{3\xi_j}{r_j^2} \theta_j \tilde{\theta}_j^3 \\ & - \sum_{j=1}^n \frac{3\xi_j}{r_j^2} \theta_j^2 \tilde{\theta}_j^2 + \sigma_n + o_3 \end{aligned} \quad (61)$$

From Lemma 6, it is obtained that

$$\sum_{j=1}^n \frac{\xi_j}{r_j^2} \tilde{\theta}_j \theta_j^3 \leq \sum_{j=1}^n \frac{3\xi_j}{r_j^2} \theta_j^2 \tilde{\theta}_j^2 + \sum_{j=1}^n \frac{\xi_j}{12r_j^2} \theta_j^4 \quad (62)$$

$$\sum_{j=1}^n \frac{3\xi_j}{r_j^2} \theta_j \tilde{\theta}_j^3 \leq \sum_{j=1}^n \frac{3\xi_j}{4\zeta^4 r_j^2} \theta_j^4 + \sum_{j=1}^n \frac{9\xi_j \zeta^{\frac{4}{3}}}{4r_j^2} \tilde{\theta}_j^4 \quad (63)$$

By substituting (62) and (63) into (61), the following formula can be seen

$$\begin{aligned} \dot{V}_n \leq & -\bar{\mu}_1 \left(\sum_{j=1}^n \frac{1}{2} z_j^2\right)^{\frac{3}{4}} - \left(\sum_{j=1}^n \frac{\eta_j}{2r_j} \tilde{\theta}_j^2\right)^{\frac{3}{4}} \\ & - \frac{\bar{\mu}_2}{n} \left(\sum_{j=1}^n \frac{1}{2} z_j^2\right)^2 + \sum_{j=1}^n \frac{\eta_j}{2r_j} \theta_j^2 + \sum_{j=1}^n \frac{\xi_j}{12r_j^2} \theta_j^4 \\ & - \sum_{j=1}^n \frac{\xi_j}{r_j^2} \tilde{\theta}_j^4 + \sum_{j=1}^n \frac{3\xi_j}{4\zeta^4 r_j^2} \theta_j^4 + \sum_{j=1}^n \frac{9\xi_j \zeta^{\frac{4}{3}}}{4r_j^2} \tilde{\theta}_j^4 \\ & + \sigma_n + o_3 \\ \leq & -\bar{\mu}_1 \left(\sum_{j=1}^n \frac{1}{2} z_j^2\right)^{\frac{3}{4}} - \check{\mu}_1 \left(\sum_{j=1}^n \frac{1}{2r_j} \tilde{\theta}_j^2\right)^{\frac{3}{4}} \\ & - \frac{\bar{\mu}_2}{n} \left(\sum_{j=1}^n \frac{1}{2} z_j^2\right)^2 - \check{\mu}_2 \sum_{j=1}^n \frac{1}{4r_j^2} \tilde{\theta}_j^4 + \Theta \end{aligned} \quad (64)$$

where $\check{\mu}_1 = (\min \{\eta_j\})^{\frac{3}{4}}$, $\check{\mu}_2 = \min \left\{ \left(4 - 9\zeta^{\frac{4}{3}}\right) \xi_j \right\}$, $\Theta = \sum_{j=1}^n \frac{\eta_j}{2r_j} \theta_j^2 + \sum_{j=1}^n \frac{\xi_j}{12r_j^2} \theta_j^4 + \sum_{j=1}^n \frac{3\xi_j}{4\zeta^4 r_j^2} \theta_j^4 + \sigma_n + o_3$.

From Lemma 4, the following formula can be obtained

$$\begin{aligned} \dot{V}_n \leq & -\bar{\mu}_1 \left(\sum_{j=1}^n \frac{1}{2} z_j^2\right)^{\frac{3}{4}} - \check{\mu}_1 \left(\sum_{j=1}^n \frac{1}{2r_j} \tilde{\theta}_j^2\right)^{\frac{3}{4}} \\ & - \frac{\bar{\mu}_2}{n} \left(\sum_{j=1}^n \frac{1}{2} z_j^2\right)^2 - \frac{\check{\mu}_2}{n} \left(\sum_{j=1}^n \frac{1}{2r_j} \tilde{\theta}_j^2\right)^2 + \Theta \end{aligned} \quad (65)$$

Denote $\mu_1 = \min \{\bar{\mu}_1, \check{\mu}_1\}$, $\mu_2 = \min \left\{ \frac{\bar{\mu}_2}{n}, \frac{\check{\mu}_2}{n} \right\}$, rearranging Lemmas 3 and 4, (65) can be corresponded to the following form

$$\begin{aligned} \dot{V}_n \leq & -\mu_1 \left(\sum_{j=1}^n \frac{1}{2} z_j^2 + \sum_{j=1}^n \frac{1}{2r_j} \tilde{\theta}_j^2\right)^{\frac{3}{4}} \\ & - \frac{\mu_2}{2n} \left(\sum_{j=1}^n \frac{1}{2} z_j^2 + \sum_{j=1}^n \frac{1}{2r_j} \tilde{\theta}_j^2\right)^2 + \Theta \\ \leq & -\mu_1 V_n^{\frac{3}{4}} - \mu_2 V_n^2 + \Theta \end{aligned} \quad (66)$$

where $\mu_2 = \frac{\check{\mu}_2}{2n}$.

3.2. Stability of closed-loop system

Theorem 1. For the asymmetric input saturated nonlinear system (10), if the adaptive law is designed in the form of (24), (38), (50), and the virtual control signal along with actual control input are designed in the form of (25), (39) and (51) respectively. Then system (1) is considered to be practical fixed time stable. The following control objectives can be achieved under the premise that Assumptions 1–3 are true:

(1) All signals in the closed-loop controlled system can be guaranteed to be bounded.

(2) The tracking error converges to an arbitrarily small neighborhood around the origin in a fixed time.

Proof. Choosing $V = V_n$ as the Lyapunov function of the closed-loop system, then we have

$$\dot{V} \leq -\mu_1 V^{\frac{3}{4}} - \mu_2 V^2 + \Theta \quad (67)$$

Based on Lemma 1 and (67), we can deduce that V is bounded. From the expression for $V = V_n$, we can further deduce that $z_i, i = 1, 2, \dots, n$ and $\tilde{\theta}_i, i = 1, 2, \dots, n$ are also bounded. At the same time, we can clearly see the boundedness of $\alpha_i, i = 1, \dots, n - 1$ and v according to their expressions. From (17), it follows that $x_i, i = 1, \dots, n$ are bounded. In summary, any signal in the closed loop system remains bounded.

Additionally, according to Lemma 1 and (67), the convergence time can be determined as follows

$$T_a \leq \frac{4}{\mu_1 \varpi} + \frac{1}{\mu_2 \varpi} \quad (68)$$

The residual set of the solution of system (67) is given by

$$x \in \left\{ V \leq \min \left\{ \left(\frac{\theta}{(1-\varpi)\mu_1} \right)^{\frac{4}{3}}, \left(\frac{\theta}{(1-\varpi)\mu_2} \right)^{\frac{1}{2}} \right\} \right\} \quad (69)$$

According to the definition of V , the following formula will be obtained

$$|y - y_d| \leq 2 \left(\frac{\theta}{(1-\varpi)\mu_1} \right)^{\frac{2}{3}} \quad (70)$$

It can be seen that by selecting appropriate constant parameters, the tracking error converges to an arbitrarily small neighborhood around the origin in a fixed time.

Remark 5. In theory, the tracking control can be achieved when the given parameters satisfy $\eta_i > 0$, $\xi_i > 0$, $\tau_i > 0$, $\tau_{i0} > 0$, $K_{i1} > 0$ and $K_{i2} > 0$. However, in practical applications, we need to choose appropriate controller design parameters in order to achieve more satisfactory control results.

4. Simulation study

To further demonstrate the availability of this control scheme, the following three simulation examples are presented in this paper.

Example 1. In order to verify the rationality of the proposed control scheme, the following form of nonlinear system with asymmetric input saturation is considered.

$$\begin{cases} \dot{x}_1 = x_2 - x_1 e^{-x_1^2} \\ \dot{x}_2 = u(v) - x_1^2 x_2^3 + \cos(x_2) - 1 \\ y = x_1 \end{cases} \quad (71)$$

where $x_i, i = 1, 2$ and y represent the system state and system output, respectively. The initial state vector is $[x_1(0), x_2(0)]^T = [0, 0]^T$. At the same time, the system input $u(v)$ is as follows

$$u(v) = \begin{cases} 10, & v \geq 10 \\ v, & -9 < v < 10 \\ -9, & v \leq -9 \end{cases} \quad (72)$$

The control strategy of the nonlinear system (71) is designed based on Theorem 1.

In the simulation, the expected target is $y_d = 0.3 \sin(t) + 0.2$ and the design parameters are selected as $r_1 = 1000$, $r_2 = 10$, $\eta_1 = \xi_1 = 0.1$, $\eta_2 = \xi_2 = \underline{g}_1 = \underline{g}_2 = K_{22} = \tau_2 = \tau_{20} = 1$, $K_{11} = K_{12} = K_{21} = 5$, $\tau_1 = 0.01$, $\tau_{10} = 0.001$, $c^- = 100$.

Figs. 2–5 display the simulation results of the nonlinear system (71). Fig. 2 shows the expected target $y_d = 0.3 \sin(t) + 0.2$ and actual output $y = x_1$. Fig. 3 displays the tracking error, which shows that the tracking error of the system converges to an arbitrarily small neighborhood around the origin with a fixed time. Fig. 4 shows the relationship between the saturation model input v and the system input $u(v)$. Fig. 5 represents the trajectory of the system state x_2 .

Example 2. To further demonstrate the superiority of this scheme in practical systems, the following Duffin-Holmes chaotic system with asymmetric input saturation is considered

$$\begin{cases} \dot{x}_1 = x_2 \\ \dot{x}_2 = u(v) + x_1 - x_2 - x_1^3 + 0.25 \cos(0.3t) \\ y = x_1 \end{cases} \quad (73)$$

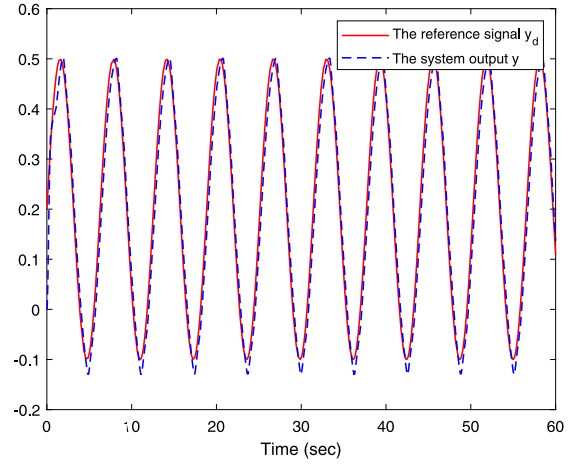


Fig. 2. The reference signal $y_d = 0.3 \sin(t) + 0.2$ and the system output y of Example 1.

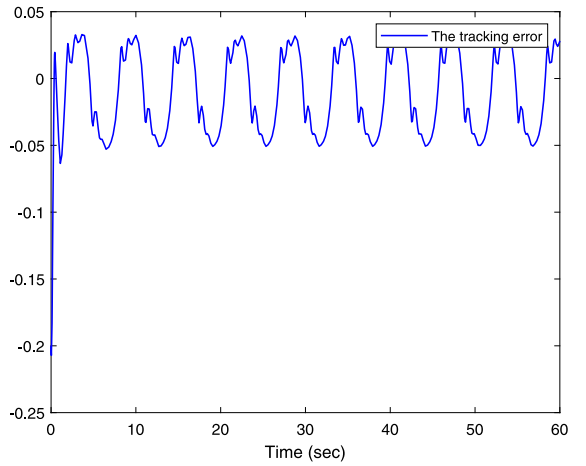


Fig. 3. The tracking error $y - y_d$ of Example 1.

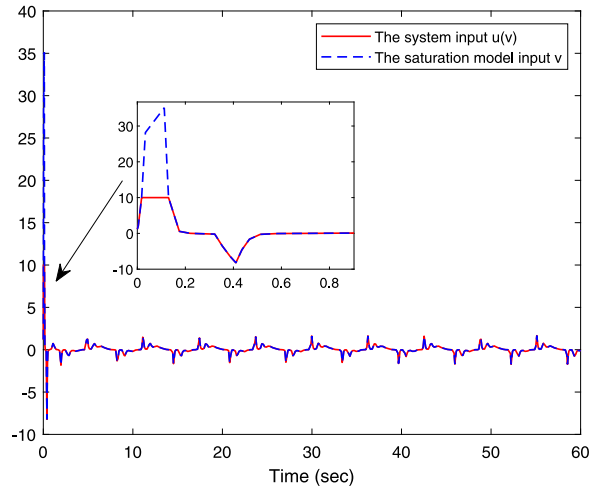


Fig. 4. The system input $u(v)$ and the saturation model input v of Example 1.

where $x_i, i = 1, 2$ and y are system states and system output, respectively. The initial state vector is $[x_1(0), x_2(0)]^T = [0, 0.25]^T$. At the same

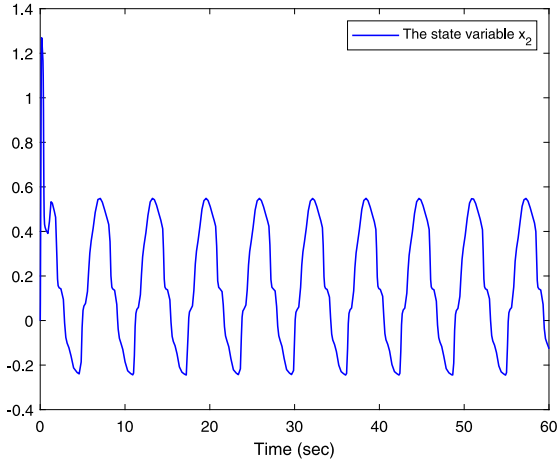


Fig. 5. The state variable x_2 of Example 1.

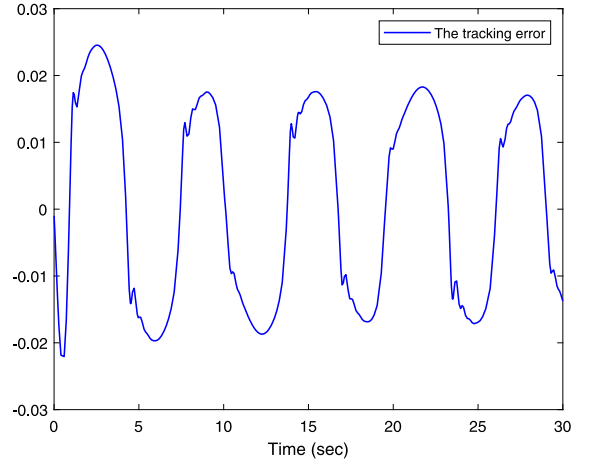


Fig. 7. The tracking error $y - y_d$ of Example 2.

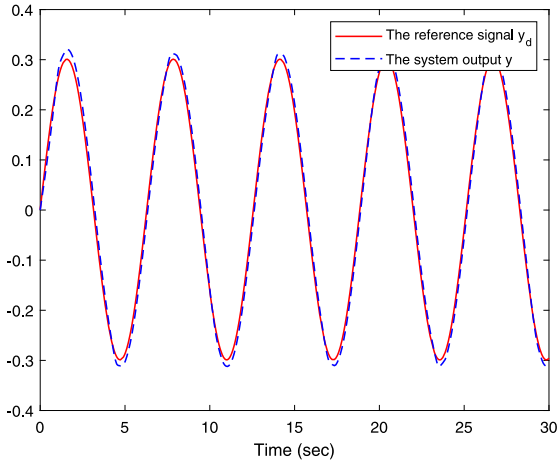


Fig. 6. The reference signal $y_d = 0.3 \sin(t) + 0.01$ and the system output y of Example 2.

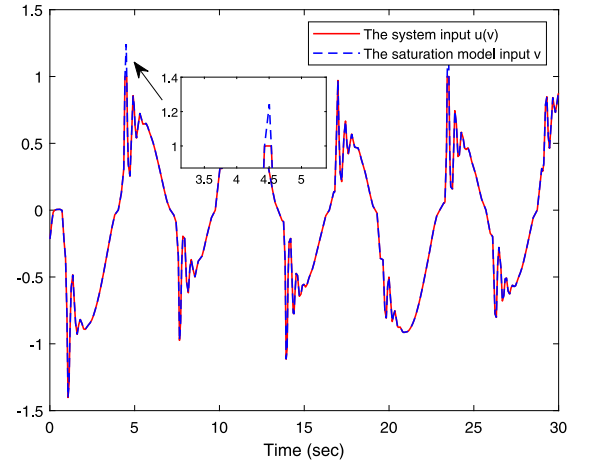


Fig. 8. The system input $u(v)$ and the saturation model input v of Example 2.

time, the input signal $u(v)$ is described as follows

$$u(v) = \begin{cases} 1, & v \geq 1 \\ v, & -3 < v < 1 \\ -3, & v \leq -3 \end{cases} \quad (74)$$

The control strategy of the nonlinear system (73) are designed based on Theorem 1.

In the simulation, the expected target is $y_d = 0.3 \sin(t) + 0.001$ and the design parameters are selected as $r_1 = 10000$, $r_2 = 10$, $\eta_1 = \xi_1 = 0.1$, $\eta_2 = \xi_2 = g_1 = g_2 = K_{22} = \tau_2 = \tau_{20} = c^- = 1$, $K_{11} = K_{12} = K_{21} = 5$, $\tau_1 = 0.01$, $\tau_{10} = 0.001$.

Figs. 6–9 display the simulation results of the nonlinear system (73). As we can see from Fig. 6, the trace scheme developed in this article is quite superior. From Fig. 7, it can be found out that the system's tracking error converges to a small neighborhood of the origin within a fixed time. Fig. 8 shows the relationship between the saturation model input v and the system input $u(v)$. Fig. 9 displays the trajectory of the system state x_2 .

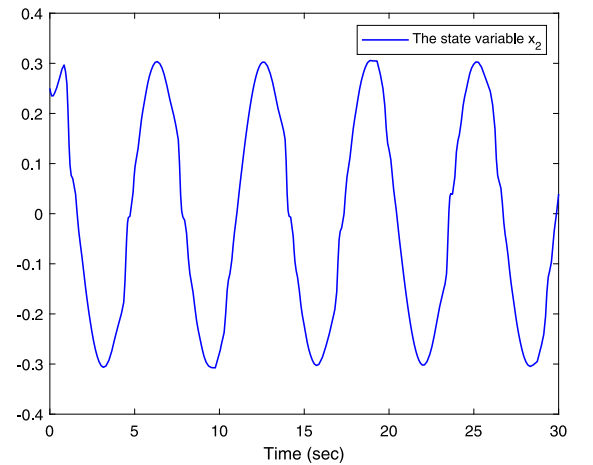


Fig. 9. The state variable x_2 of Example 2.

Example 3. In order to further verify the superiority of the control scheme proposed in this paper, a comparative experiments is introduced for system (71). The specific approach is to replace the MTN with radial basis function neural network (RBFNN) in the control structure. The simulation results are shown in Fig. 10.

It can be seen from Fig. 10 that both control strategies can achieve satisfactory tracking control effects. However, the control method proposed in this article has better control effects and requires less computation. In other words, the control method proposed in this article can achieve better control effects at a lower cost.

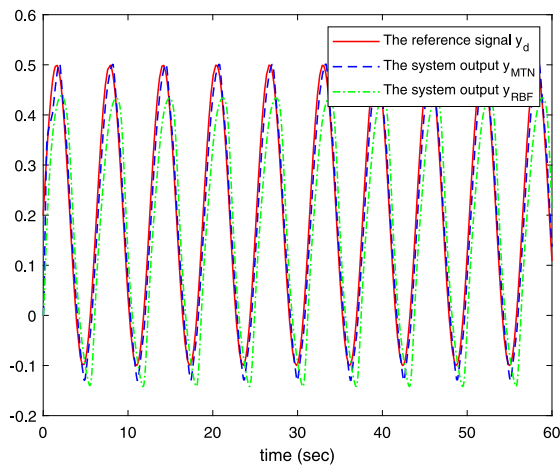


Fig. 10. Tracking trajectories of two different control strategies of Example 3.

5. Conclusion

The issue of fixed time control for nonlinear systems subject to asymmetric input saturation is discussed. Firstly, the saturated model is transformed into a linear model with bounded perturbation by constructing auxiliary function. Secondly, a new adaptive control strategy is invented by combining fixed time control with MTN. It effectively solves the problem that the finite time control cannot get rid of the initial state. Finally, three examples illustrate the feasibility of the scheme.

CRediT authorship contribution statement

Ya-Feng Zhou: Formal analysis, Methodology, Software, Writing – original draft. **Shan-Liang Zhu:** Formal analysis, Supervision, Writing – original draft. **Wei Zhao:** Formal analysis, Software. **Yu-Qun Han:** Formal analysis, Funding acquisition, Methodology, Software, Writing – review & editing.

Declaration of competing interest

The authors declare that they have no known competing financial interests or personal relationships that could have appeared to influence the work reported in this paper.

Data availability

Data sharing not applicable to this article as no datasets were generated or analysed during the current study.

References

- Ba, D.-S., Li, Y.-X., & Tong, S.-C. (2019). Fixed-time adaptive neural tracking control for a class of uncertain nonstrict nonlinear systems. *Neurocomputing*, 363, 273–280. <http://dx.doi.org/10.1016/j.neucom.2019.06.063>.
- Chen, M., Wang, H.-Q., & Liu, X. P. (2021). Adaptive practical fixed-time tracking control with prescribed boundary constraints. *IEEE Transactions on Circuits and Systems. I. Regular Papers*, 68(4), 1716–1726. <http://dx.doi.org/10.1109/TCSI.2021.3051076>.
- Du, Y., Zhu, S.-L., Zhai, L.-L., & Han, Y.-Q. (2023). Switching threshold-based event-triggered adaptive asymptotic tracking control for stochastic nonlinear systems with full-state constraints. *International Journal of Robust and Nonlinear Control*, 33(13), 7908–7928. <http://dx.doi.org/10.1002/rnc.6803>.
- Gao, Y.-F., Sun, X.-M., Wen, C.-Y., & Wang, W. (2017). Adaptive tracking control for a class of stochastic uncertain nonlinear systems with input saturation. *IEEE Transactions on Automatic Control*, 62(5), 2498–2504. <http://dx.doi.org/10.1109/TAC.2016.2600340>.

- Han, Y.-Q., Li, N., He, W.-J., & Zhu, S.-L. (2021). Adaptive multi-dimensional Taylor network funnel control of a class of nonlinear systems with asymmetric input saturation. *International Journal of Adaptive Control and Signal Processing*, 35(5), 713–726. <http://dx.doi.org/10.1002/acs.3224>.
- He, W.-J., Zhu, S.-L., Li, N., & Han, Y.-Q. (2023). Adaptive finite-time control for switched nonlinear systems subject to multiple objective constraints via multi-dimensional Taylor network approach. *ISA Transactions*, 136, 323–333. <http://dx.doi.org/10.1016/j.isatra.2022.10.048>.
- He, W.-J., Zhu, S.-L., Li, N., & Han, Y.-Q. (2023a). Adaptive controller design for switched stochastic nonlinear systems subject to unknown dead-zone input via new type of network approach. *International Journal of Control, Automation and Systems*, 21, 499–507. <http://dx.doi.org/10.1007/s12555-021-0860-z>.
- He, W.-J., Zhu, S.-L., Lu, L.-T., & Han, Y.-Q. (2024). A novel network-based adaptive fault-tolerant control of switched nonlinear systems subject to multiple faults under prescribed performance. *ISA Transactions*, 145, 78–86. <http://dx.doi.org/10.1016/j.isatra.2023.12.008>.
- Jayaprakash, A. K., & Mackunis, W. (2022). Nonlinear adaptive control of fluid flow dynamic systems under actuator uncertainty. In *IEEE conference on control technology and applications*. <http://dx.doi.org/10.1109/CCTA49430.2022.9966108>.
- Jin, X. (2019). Adaptive fixed-time control for MIMO nonlinear systems with asymmetric output constraints using universal barrier functions. *IEEE Transactions on Automatic Control*, 64(7), 3046–3053. <http://dx.doi.org/10.1109/TAC.2018.2874877>.
- Kang, A.-M., & Yan, H.-S. (2022). Asymptotic tracking and dynamic regulation of MIMO nonaffine nonlinear system with actuator saturation via multidimensional Taylor network controller. *IEEE Transactions on Systems, Man, and Cybernetics: Systems*, 52(8), 4937–4949. <http://dx.doi.org/10.1109/TSMC.2021.3106314>.
- Lensvelt, R., Speetjens, M. F. M., & Nijmeijer, H. (2022). Fast fluid heating by adaptive flow reorientation. *International Journal of Thermal Sciences*, 180, Article 107720. <http://dx.doi.org/10.1016/j.ijthermalsci.2022.107720>.
- Li, H.-Y., Bai, L., Zhou, Q., Lu, R.-Q., & Wang, L.-J. (2017). Adaptive fuzzy control of stochastic nonstrict-feedback nonlinear systems with input saturation. *IEEE Transactions on Systems, Man, and Cybernetics: Systems*, 47(8), 2185–2197. <http://dx.doi.org/10.1109/TSMC.2016.2635678>.
- Li, N., Han, Y.-Q., He, W.-J., & Zhu, S.-L. (2022). Control design for stochastic nonlinear systems with full-state constraints and input delay: a new adaptive approximation method. *International Journal of Control, Automation and Systems*, 20, 2768–2778. <http://dx.doi.org/10.1007/s12555-021-0451-z>.
- Li, Y.-M., Tong, S.-C., & Li, T.-S. (2016). Hybrid fuzzy adaptive output feedback control design for uncertain MIMO nonlinear systems with time-varying delays and input saturation. *IEEE Transactions on Fuzzy Systems*, 24(4), 841–853. <http://dx.doi.org/10.1109/TFUZZ.2015.2486811>.
- Li, M., & Xiang, Z.-R. (2019). Adaptive neural network tracking control for a class of switched nonlinear systems with input delay. *Neurocomputing*, 366, 284–294. <http://dx.doi.org/10.1016/j.neucom.2019.08.011>.
- Li, N., Zhu, S.-L., He, W.-J., & Han, Y.-Q. (2022). Controller design for nonlinear systems subject to both input saturation and asymmetry time-varying state constraints: A novel network-based approach. *International Journal of Adaptive Control and Signal Processing*, 36(12), 3124–3141. <http://dx.doi.org/10.1002/acs.3503>.
- Liu, L., Gao, T.-T., Liu, Y.-J., & Tong, S.-C. (2020). Time-varying asymmetrical BLFs based adaptive finite-time neural control of nonlinear systems with full state constraints. *IEEE/CAA Journal of Automatica Sinica*, 7(5), 1335–1343. <http://dx.doi.org/10.1109/JAS.2020.1003213>.
- Liu, J., Yu, Y., He, H.-B., & Sun, C.-Y. (2021). Team-triggered practical fixed-time consensus of double-integrator agents with uncertain disturbance. *IEEE Transactions on Cybernetics*, 6(51), 3263–3272. <http://dx.doi.org/10.1109/TCYB.2020.2999199>.
- Ma, J.-J., Ge, S.-Z. S., Zheng, Z.-Q., & Hu, D.-W. (2015). Adaptive NN control of a class of nonlinear systems with asymmetric saturation actuators. *IEEE Transactions on Neural Networks and Learning Systems*, 26(7), 1532–1538. <http://dx.doi.org/10.1109/TNNLS.2014.2344019>.
- McAllister, R. D., & Rawlings, J. B. (2023). Nonlinear stochastic model predictive control: Existence, measurability, and stochastic asymptotic stability. *IEEE Transactions on Automatic Control*, 68(3), 1524–1536. <http://dx.doi.org/10.1109/TAC.2022.3157131>.
- Mesbah, A. (2016). Stochastic model predictive control: An overview and perspectives for future research. *IEEE Control Systems Magazine*, 36(6), 30–44. <http://dx.doi.org/10.1109/MCS.2016.2602087>.
- Ning, B.-D., Han, Q.-L., & Zuo, Z.-Y. (2019). Practical fixed-time consensus for integrator-type multi-agent systems: A time base generator approach. *Automatica*, 105, 406–414. <http://dx.doi.org/10.1016/j.automatica.2019.04.013>.
- Polyakov, A., Efimov, D., & Perruquetti, W. (2015). Finite-time and fixed-time stabilization: Implicit Lyapunov function approach. *Automatica*, 51, 332–340. <http://dx.doi.org/10.1016/j.automatica.2014.10.082>.
- Saravanan, S., & Meenasaranya, M. (2018). Lyapunov stability of plane parallel porous convection with heat generation. *Meccanica*, 53, 497–501. <http://dx.doi.org/10.1007/s11012-017-0750-x>.
- Saravanan, S., & Meenasaranya, M. (2022). Unconditional stability of an externally controlled medium with thermodynamic non-equilibrium. *Zeitschrift für Angewandte Mathematik und Physik*, 73, 206. <http://dx.doi.org/10.1007/s00033-022-01843-4>.

- Sun, W.-J., Gao, M.-M., & Zhao, J.-S. (2022). Adaptive fuzzy finite-time control for a class of stochastic nonlinear systems with input saturation. *International Journal of Fuzzy Systems*, 24, 265–275. <http://dx.doi.org/10.1007/s40815-021-01107-9>.
- Sun, W., Su, S.-F., Wu, Y.-Q., & Xia, J.-W. (2021). Novel adaptive fuzzy control for output constrained stochastic nonstrict feedback nonlinear systems. *IEEE Transactions on Fuzzy Systems*, 29(5), 1188–1197. <http://dx.doi.org/10.1109/TFUZZ.2020.2969909>.
- Tao, F.-Z., Fan, P.-Y., Fu, Z.-M., Wang, N., & Wang, Y.-Y. (2022). Adaptive fuzzy fixed time control for pure-feedback stochastic nonlinear systems with full state constraints. *Journal of the Franklin Institute*, 359(10), 4642–4660. <http://dx.doi.org/10.1016/j.jfranklin.2022.05.007>.
- Wang, L.-J., & Chen, C. L. P. (2021). Reduced-order observer-based dynamic event-triggered adaptive NN control for stochastic nonlinear systems subject to unknown input saturation. *IEEE Transactions on Neural Networks and Learning Systems*, 32(4), 1678–1690. <http://dx.doi.org/10.1109/TNNLS.2020.2986281>.
- Wang, H.-Q., Chen, B., & Lin, C. (2014). Adaptive neural tracking control for a class of stochastic nonlinear systems. *International Journal of Robust and Nonlinear Control*, 24(7), 1262–1280. <http://dx.doi.org/10.1002/rnc.2943>.
- Wang, F., Chen, B., Lin, C., Zhang, J., & Meng, X.-Z. (2018). Adaptive neural network finite-time output feedback control of quantized nonlinear systems. *IEEE Transactions on Cybernetics*, 48(6), 1839–1848. <http://dx.doi.org/10.1109/TCYB.2017.2715980>.
- Wang, H.-Q., Chen, M., & Liu, X.-P. (2021). Fuzzy adaptive fixed-time quantized feedback control for a class of nonlinear systems. *Acta Automatica Sinica*, 47(12), 2823–2830. <http://dx.doi.org/10.16383/j.aas.c190681>.
- Wang, H.-Q., Chen, B., Liu, X.-P., Liu, K.-F., & Lin, C. (2014). Adaptive neural tracking control for stochastic nonlinear strict-feedback systems with unknown input saturation. *Information Sciences*, 269, 300–315. <http://dx.doi.org/10.1016/j.ins.2013.09.043>.
- Wang, D.-M., Han, Y.-Q., Lu, L.-T., & Zhu, S.-L. (2024). Dynamic event-triggered adaptive tracking control for stochastic nonlinear systems with deferred time-varying constraints. *Chaos, Solitons & Fractals*, 182, Article 114814. <http://dx.doi.org/10.1016/j.chaos.2024.114814>.
- Wang, C.-L., & Lin, Y. (2015). Decentralized adaptive tracking control for a class of interconnected nonlinear time-varying systems. *Automatica*, 54, 16–24. <http://dx.doi.org/10.1016/j.automatica.2015.01.041>.
- Wang, H.-Q., Wen, B., & Liu, P.-X.-P. (2019). Finite-time adaptive fault-tolerant control for nonlinear systems with multiple faults. *IEEE/CAA Journal of Automatica Sinica*, 6(6), 1417–1427. <http://dx.doi.org/10.1109/JAS.2019.1911765>.
- Wang, G.-B., Yan, H.-S., & Zheng, X.-Y. (2023a). Contraction-based stochastic model predictive control for nonlinear systems with input delay using multidimensional Taylor network. *IEEE Transactions on Automatic Control*, 68(12), 7498–7513. <http://dx.doi.org/10.1109/TAC.2023.3281349>.
- Wang, M.-X., Zhu, S.-L., Liu, S.-M., Du, Y., & Han, Y.-Q. (2023b). Design of adaptive finite-time fault-tolerant controller for stochastic nonlinear systems with multiple faults. *IEEE Transactions on Automation Science and Engineering*, 20(4), 2492–2502. <http://dx.doi.org/10.1109/TASE.2022.3206328>.
- Wen, C.-Y., Zhou, J., Liu, Z. T., & Su, H.-Y. (2011). Robust adaptive control of uncertain nonlinear systems in the presence of input saturation and external disturbance. *IEEE Transactions on Automatic Control*, 56(7), 1672–1678. <http://dx.doi.org/10.1109/TAC.2011.2122730>.
- Wu, J.-H., Jin, Z.-H., Liu, A.-D., Yu, L., & Yang, F.-W. (2024). A hierarchical data-driven predictive control of image-based visual servoing systems with unknown dynamics. *IEEE Transactions on Cybernetics*, 54(5), 3160–3173. <http://dx.doi.org/10.1109/TCYB.2022.3228123>.
- Wu, J.-H., & Yang, F.-W. (2023). A dual-driven predictive control for photovoltaic-diesel microgrid secondary frequency regulation. *Applied Energy*, 334, Article 120652. <http://dx.doi.org/10.1016/j.apenergy.2023.120652>.
- Xu, H., Yu, D.-X., Sui, S., Zhao, Y.-P., Chen, C. L. P., & Wang, Z. (2023). Nonsingular practical fixed-time adaptive output feedback control of MIMO nonlinear systems. *IEEE Transactions on Neural Networks and Learning Systems*, 34(10), 7222–7234. <http://dx.doi.org/10.1109/TNNLS.2021.3139230>.
- Yang, T., Sun, N., & Fang, Y.-C. (2022). Adaptive fuzzy control for a class of MIMO underactuated systems with plant uncertainties and actuator deadzones: design and experiments. *IEEE Transactions on Cybernetics*, 52(8), 8213–8226. <http://dx.doi.org/10.1109/TCYB.2021.3050475>.
- Zhang, T., Ge, S.-S., & Hang, C.-C. (2000). Adaptive neural network control for strict-feedback nonlinear systems using backstepping design. *Automatica*, 36(12), 1835–1846. [http://dx.doi.org/10.1016/S0005-1098\(00\)00116-3](http://dx.doi.org/10.1016/S0005-1098(00)00116-3).
- Zhou, Y.-F., Zhao, W., Zhu, S.-L., Han, Y.-Q., Xing, J.-M., & Zhou, Q.-H. (2024). Multi-dimensional Taylor network-based adaptive fixed-time tracking control for a class of nonlinear systems with input delay. *International Journal of Control*, <http://dx.doi.org/10.1080/00207179.2024.2319752>.
- Zhu, S.-L., & Han, Y.-Q. (2022). Adaptive decentralized prescribed performance control for a class of large-scale nonlinear systems subject to nonsymmetric input saturations. *Neural Computing and Applications*, 34(13), 11123–11140. <http://dx.doi.org/10.1007/s00521-022-07032-8>.
- Zuo, Z.-Y. (2015). Non-singular fixed-time terminal sliding mode control of non-linear systems. *IET Control Theory & Applications*, 9(4), 545–552. <http://dx.doi.org/10.1049/iet-cta.2014.0202>.
- Zuo, Z.-Y., Tian, B.-L., Defoort, M., & Ding, Z.-T. (2018). Fixed-time consensus Tracking for multi-agent systems with high-order integrator dynamics. *IEEE Transactions on Automatic Control*, 63(2), 563–570. <http://dx.doi.org/10.1109/TAC.2017.2729502>.